

Article

Experimental Investigation on Fire Smoke Temperature under Forced Ventilation Conditions in a Bifurcated Tunnel with Fires Situated in a Branch Tunnel

Hanwen Guo, Zhengyuan Yang, Peiyao Zhang, Yunji Gao * and Yuchun Zhang *

Department of Fire Protection Engineering, Southwest Jiaotong University, Chengdu 610031, China; hanwenguo@my.swjtu.edu.cn (H.G.); yangzy999@my.swjtu.edu.cn (Z.Y.); zpy2021211870@my.swjtu.edu.cn (P.Z.)
* Correspondence: gjy119@swjtu.edu.cn (Y.G.); zycfire@home.swjtu.edu.cn (Y.Z.)

Abstract: In this work, a number of experiments were conducted in a reduced scale bifurcation tunnel with a ratio of 1:10 to explore the influence of the position of longitudinal fires (placed in branch tunnel) on smoke temperature profile under forced ventilation. Three heat release rates, six ventilation velocities, and three fire locations were considered. The main findings are summarized below, as follows: The temperature of smoke downstream of the main tunnel decreases with the rate of ventilation and longitudinal fire location. In contrast, the smoke temperature downstream of the fire source inside the branch tunnel drops with the ventilation velocity; the maximum temperature of the flame under the ceiling of the tunnel rises with longitudinal fire location. The dimensionless longitudinal smoke temperatures downstream of the main tunnel decrease exponentially with longitudinal distance, and the same observation is found in the branch tunnel. The attenuation coefficient k in the main tunnel increases with longitudinal ventilation velocity according to a power law but does not change significantly with longitudinal fire locations. However, the exponential coefficient k' in the branch tunnel decreases linearly with ventilation velocity, whereas it increases with longitudinal fire location inside the branch tunnel. Lastly, modified models are established for estimating the longitudinal profile of temperatures downstream of the main tunnel and branch tunnel, where the influence of the rate of ventilation and location of the fire are taken into account.

Keywords: bifurcated tunnel; fire location; forced ventilation; temperature distribution of smoke; tunnel fire



Citation: Guo, H.; Yang, Z.; Zhang, P.; Gao, Y.; Zhang, Y. Experimental Investigation on Fire Smoke Temperature under Forced Ventilation Conditions in a Bifurcated Tunnel with Fires Situated in a Branch Tunnel. *Fire* **2023**, *6*, 473. <https://doi.org/10.3390/fire6120473>

Academic Editor: Tiago Miguel Ferreira

Received: 23 October 2023
Revised: 23 November 2023
Accepted: 4 December 2023
Published: 17 December 2023



Copyright: © 2023 by the authors. Licensee MDPI, Basel, Switzerland. This article is an open access article distributed under the terms and conditions of the Creative Commons Attribution (CC BY) license (<https://creativecommons.org/licenses/by/4.0/>).

1. Introduction

Tunnel construction can be destroyed by high-temperature smoke produced by a tunnel fire, and, in these situations, the accumulation and propagation of hot smoke can make evacuation arduous. Meanwhile, smoke is a huge challenge to the extinguishing and controlling of a fire, which may lead to immeasurable loss of personnel and property. For instance, 38 people were killed in the Mont Blanc tunnel fire after baking for 53 h in a scorching heat [1], and the Futuyu Tunnel fire in China resulted in 15 fatalities and three injuries [2]. Therefore, smoke characteristics, especially temperature distribution, have been investigated widely as a classical problem [3–10]. However, previous research mostly concentrated on the influences of longitudinal ventilation [11–13], sealing ratio [14–16] and fire location [17–19] on temperature profile in single tunnels. In addition, full-scale fire tests of battery-electric vehicles were conducted to investigate fire behavior, and new approaches to fighting a BEV fire were suggested [20]. In addition to experimental studies, the numerical simulation approach is also a common method used to investigate tunnel fires, for example FDS [21] and Large Eddy Simulations [22]. In the past few years, with the acceleration of urbanization, tunnel structure has become increasingly complicated. A bifurcated tunnel, one of said complex tunnels, can be understood as a tunnel structure composed of a main tunnel and a branch tunnel, commonly used in tunnel traffic conversion

belts and urban connection tunnels [23]. Figure 1a–c demonstrate that smoke dynamics and smoke movements of a fire ignited in a bifurcated tunnel are more complex than when a fire develops in a conventional single tunnel.

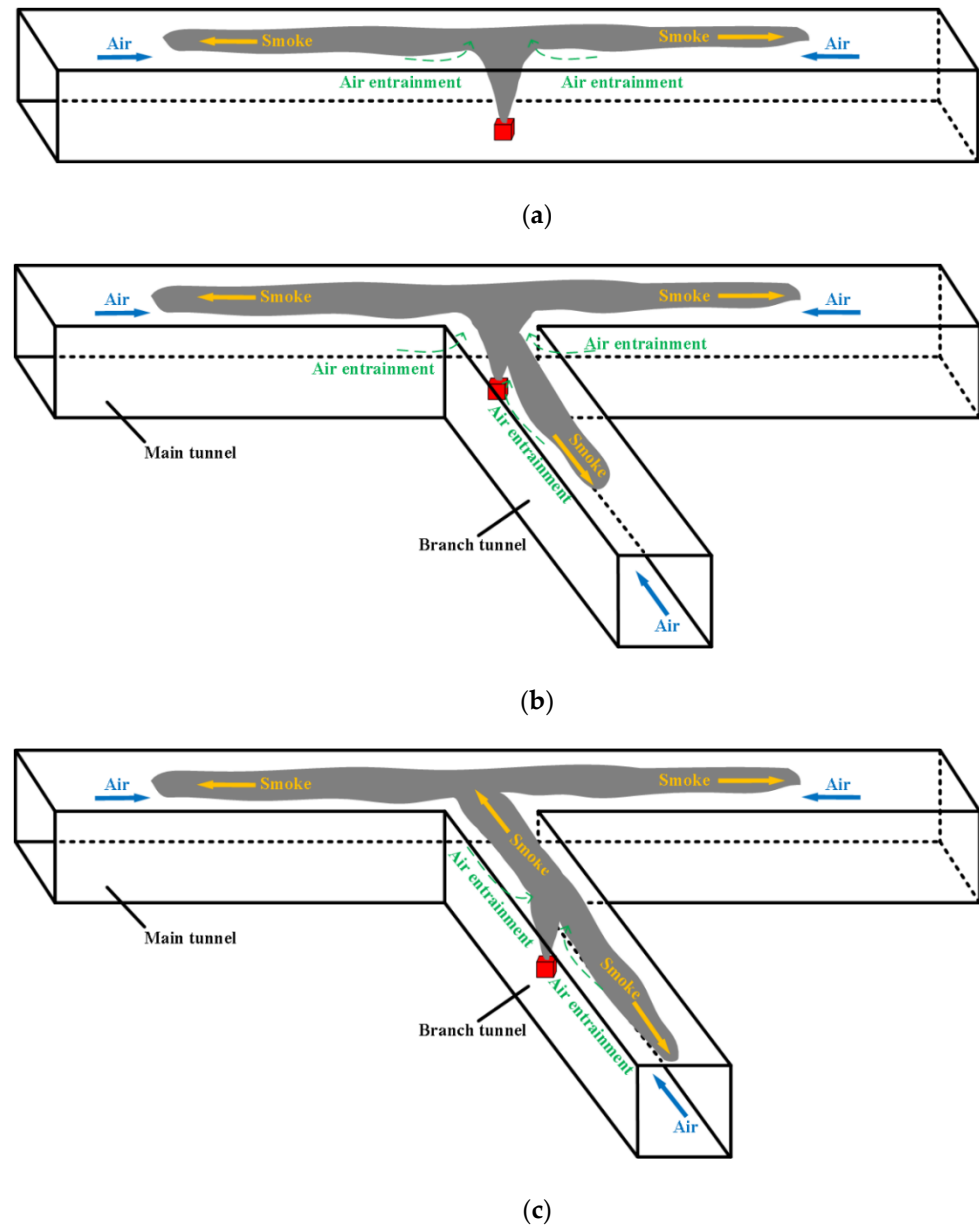


Figure 1. Differences in smoke flow between conventional single-bore tunnels and bifurcated tunnels: (a) smoke flow in a conventional single-bore tunnel; (b) smoke flow in a bifurcated tunnel (fires occurred in the main tunnel); (c) smoke flow in a bifurcated tunnel (fires occurred in the branch tunnel).

As a result, a bifurcation tunnel will have a different temperature profile from a conventional single tunnel [24,25], which leads to new problems and challenges in tunnel safety. Therefore, a study of the temperature distribution of smoke in bifurcated tunnel fires is necessary.

As is well known, a longitudinal ventilation system is extensively used as a smoke exhaust system in tunnel fires, where it is applied to control the smoke and guarantee life safety. The profile of the temperature of a tunnel ceiling under longitudinal ventilation conditions has been both theoretically and practically investigated by Li [8], Hu [9],

Tang [26], Li [27], and Zhao [13]. Moreover, the impact of longitudinal ventilation on flame smoke back-layering length [11,28,29] and critical velocity [30,31] have also been extensively investigated. Kurioka et al. [32] proposed a model for predicting the maximum temperature rise in tunnels under the effect of longitudinal ventilation, and verified the prediction results of the model through reduced-scale tunnel fire experiments. Wu and Bakar [33] investigated the effect of different tunnel cross-sectional areas on the critical wind velocity using reduced-scale experiments, and predicted the critical wind velocity for ventilation and smoke extraction. Unfortunately, the above studies have mainly focused on the characteristics of smoke in conventional single tunnel fires, while relatively few research results have been conducted for bifurcated tunnel fires.

In recent years, bifurcated tunnel fire has increasingly gained significant attention.

Lei et al. [34] conducted small-scale experiments to investigate the longitudinal ventilation for fire in a branched tunnel, and proposed two critical ventilation modes for different rates of ventilation in the branch and the main tunnel with its fire source arranged at the tunnel intersection. Chen et al. [35] experimentally studied the distributions of peak temperature increases and the distribution of heat flux longitudinally below the ceiling under multidirectional ventilation. A model was developed to evaluate the peak temperature increase below the tunnel ceiling inside a bifurcated tunnel, under multi-directional ventilation. Tao et al. [36] conducted a number of reduced-model tests in a two-part tunnel to investigate the change in maximum temperature, temperature decay, and smoke spread under conditions of ventilation of the upstream tunnel section. Chen et al. [37,38] compared the differences between ordinary tunnel fire and bifurcated tunnel fire and investigated the profile of temperature in a bifurcated tunnel affected by the effect of a ramp slope. It was found that the existence of a bifurcated tunnel would result in a smaller maximum ceiling temperature than a single tunnel above the fire source and that the longitudinal temperature in the main tunnel will increase with the ramp slope. Liu et al. [25] experimentally analyzed the smoke temperature of a subway tunnel connection area considering the uphill and downhill slope effect, and the dimensionless temperature profiles were proved to be mainly linked to the slopes of the current tunnel. Moreover, Liu et al. [39] evaluated the temperature of smoke under the influence of a transverse fire source position in bifurcated tunnel fires and proposed an adjusted model for forecasting temperature profile of a transverse and longitudinal direction. Lei et al. [2] discovered that, while the fire source is placed at the tunnel's intersection, the maximum flame temperature under the tunnel ceiling is a little lower than the temperature of the fire elsewhere in the main tunnel. Li et al. [40] noted that the longitudinal temperature in the main tunnel raises first and then reduces as the distance of the fire source from the sidewall grows by studying the impact of transverse fire locations in a main tunnel. From a set of longitudinally ventilated bifurcated tunnel combustion experiments, Chen et al. [41] found that the flue gas temperature under the tunnel roof decreases as the rate of longitudinal ventilation increases. The maximum smoke temperature is significantly influenced by the bifurcation angle under forced ventilation according to the research on the impact of the angle of bifurcation on the distribution of smoke temperature under natural and forced ventilations of Huang et al. [42]. Moreover, a predicted model was put forth for maximum excess temperature considering the bifurcation angle and forced ventilation. At present, there are few studies focusing on the impact of longitudinal ventilation on fire characteristics in bifurcated tunnels, especially on cases in which the fire occurred in a branch tunnel. Therefore, it is imperative to research the role of a fire's position in affecting the longitudinal distribution of smoke temperature with forced ventilation in a bifurcated tunnel.

A variety of experiments were carried out in the current work in a 1:10 reduced-scale bifurcated tunnel to explore the impact of fire location on the distribution of smoke temperature under conditions of fires in a bifurcated tunnel with a longitudinal airflow. The variables of fire location, longitudinal ventilation, and heat release rate of fire were considered. In this paper, the smoke temperature profile is analyzed and compared, and a predicted model for the temperature profile of smoke in bifurcated tunnel fires is proposed,

taking the impact of fire location and longitudinal ventilation into account. Therefore, the conclusions drawn in this work are not only practical in fire prevention and in the control of bifurcated tunnel fires, but also provide more basic theoretical information for future research.

2. Experiment Setup

A reduced-scale bifurcated tunnel with a ratio of 1:10 served as the experimental device, as illustrated in Figure 2a, a model which has been used in previous studies [40,41,43]. The bifurcated tunnel [44,45] is composed of a main tunnel and a branch tunnel. The conjunction area is located between the 4.5 m and the 5.5 m of the main tunnel. The lengths of the main and branch tunnels are, respectively, 10.0 m and 5.0 m. In addition, the cross-section of the bifurcated tunnel is 1.0 m in width and 0.6 m in height. The angle between the main and branch tunnels is set to 45°. The longitudinal ventilation rate in the tunnel is controlled by altering the frequency using a fan with adjustable wind velocity installed at the left entrance of the main tunnel. In addition, the experimental tunnel is built based on Froude's scaling law, which is applied extensively in reduced-scale experiments to fit real-scale models. The law can be expressed as follows [46]:

$$\frac{Q_r}{Q_f} = \left(\frac{l_r}{l_f}\right)^{\frac{5}{2}} \quad (1)$$

$$\frac{t_r}{t_f} = \left(\frac{l_r}{l_f}\right)^{\frac{1}{2}} \quad (2)$$

$$T_r = T_f \quad (3)$$

where Q represents the heat release rate of the fire; t represents the burning duration; T represents the temperature of the flame; subscript f represents the full-scale model parameters, and r represents the reduced-scale model parameters.

The size of the burner used in this work was 0.2 m × 0.2 m × 0.2 m, and liquefied petroleum gas was selected to ignite it, which has been widely used in previous work [40,42,43]. Three kinds of heat release rates (HRR) of 15.9 kW, 23.9 kW, and 31.9 kW were designed. The fire was arranged on the centerline in the tunnels that branch off, and the longitudinal distances (D) of the ignition source from the bifurcated junction were 0.5 m, 1.0 m, and 1.5 m, respectively. Also being taken into account were the longitudinal ventilation rate (V), including 0 ms⁻¹, 0.45 ms⁻¹, 0.6 ms⁻¹, 0.75 ms⁻¹, 1.0 ms⁻¹, and 1.3 ms⁻¹. The experimental conditions of ambient temperature and pressure were 18°C and 101 kPa, respectively. Table 1 includes all the experimental situations. In this work, two or three repetitive tests were carried out for each set of conditions.

Table 1. Experimental conditions in this work.

Test No.	HRR (kW)	D (m)	V (ms ⁻¹)
1–18	15.9	0.5, 1.0, 1.5	0, 0.45, 0.6, 0.75, 1.0, 1.3
19–36	23.9	0.5, 1.0, 1.5	0, 0.45, 0.6, 0.75, 1.0, 1.3
37–54	31.9	0.5, 1.0, 1.5	0, 0.45, 0.6, 0.75, 1.0, 1.3

In order to detect the smoke temperature, several thermocouples were arranged in the tunnel as displayed in Figure 2b. Five thermocouple trees with an interval of 0.2 m were placed within a square with sides of 1.0 m at the intersection of the main tunnel (M₁~M₅) and the bifurcated tunnel (B₁~B₅), and each thermocouple tree was made up of eleven thermocouples, with an interval of 0.1 m. A set of thermocouples were spaced at 0.25 m intervals along the center line of the main tunnel on the left and right sides of the intersection (J₁ and J₂), respectively, which was encrypted with an interval of 0.1 m

in some parts. Another set of thermocouples (J_3) was positioned at intervals of 0.1 and 0.5 m following the center line of the branch tunnel. In order to ensure that the temperature measured by the thermocouple was close to the highest temperature of the flue gas in the vertical direction, the thermocouples were arranged 2 cm beneath the ceiling of the main tunnel and the branch tunnel, which is similar to previous works [35]. All the thermocouples used in this work, with a diameter of 1.5 mm, had a response time of 0.03 s and a temperature measurement range of 0 °C to 1200 °C. Before each experiment, the accuracy of all thermocouples was calibrated by detecting boiling water, and the standard of measurement tolerance was less than 3% [5,40]. According to Froude's similarity criterion, the heat release rates of the single fires in this scaling experiment were converted to the full-scale experimental values of 5.04 MW, 7.56 MW, and 10.08 MW, respectively. In addition, the corresponding longitudinal ventilation velocity values in a full-scale experiment were 0 m/s, 1.43 m/s, 1.9 m/s, 2.38 m/s, 3.17 m/s, and 4.12 m/s, obtained by converting the longitudinal ventilation velocities in our reduced-scale experiment.

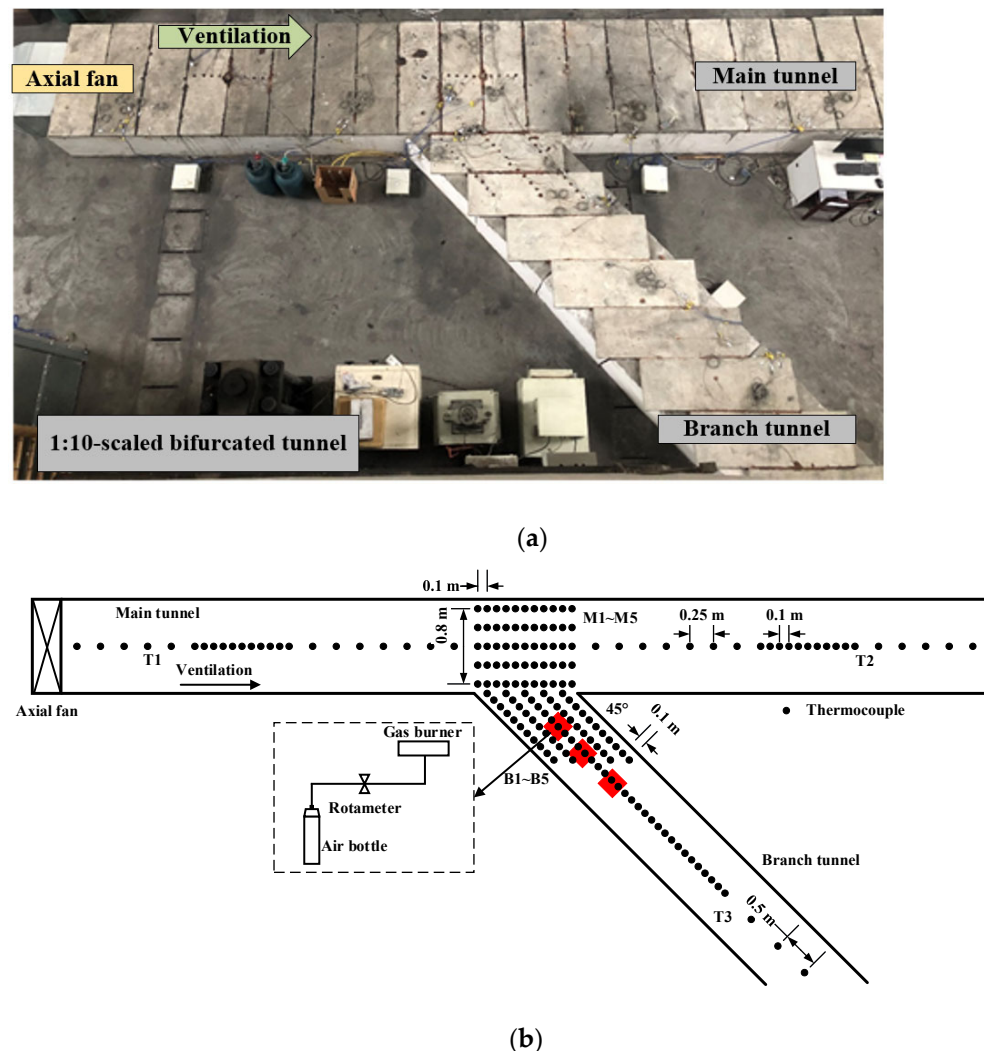


Figure 2. Schematic diagram of a 1:10 small-scale tunnel: (a) 1:10-scaled bifurcated tunnel model; (b) arrangement of thermocouples.

3. Results and Discussion

3.1. Summary of the Results of the Experiment

Figure 3 shows the temperature profile of smoke at the junction region under different fire source locations and ventilation velocities, with HRR = 15.9 kW. It can be seen from Figure 3 that, for no longitudinal ventilation conditions, the smoke will move upstream

in the main tunnel, where the smoke flows into the junction of the main tunnel due to the special structure of a bifurcated tunnel. However, as V increases, the smoke is gradually blown downstream. Moreover, for fixed D conditions, the maximum smoke temperature at the bifurcation junction decreases with the increase in V . It is remarkable that the position of the fire source also affects the smoke flux path and the temperature distribution at the bifurcation junction. Notably, for fixed $D = 0.5$ m conditions, the smoke moves upstream in the main tunnel with $V < 0.75$ ms^{-1} , whereas the smoke is blown downstream when $V = 1.30$ ms^{-1} . Meanwhile, for fixed $D = 1.5$ m conditions, the smoke moves upstream in the main tunnel with no ventilation, but flows downstream with $V > 0.45$ ms^{-1} . Moreover, under a fixed longitudinal ventilation, the more distant the fire source is from the junction, the lower the temperature is in the junction region in the main tunnel.

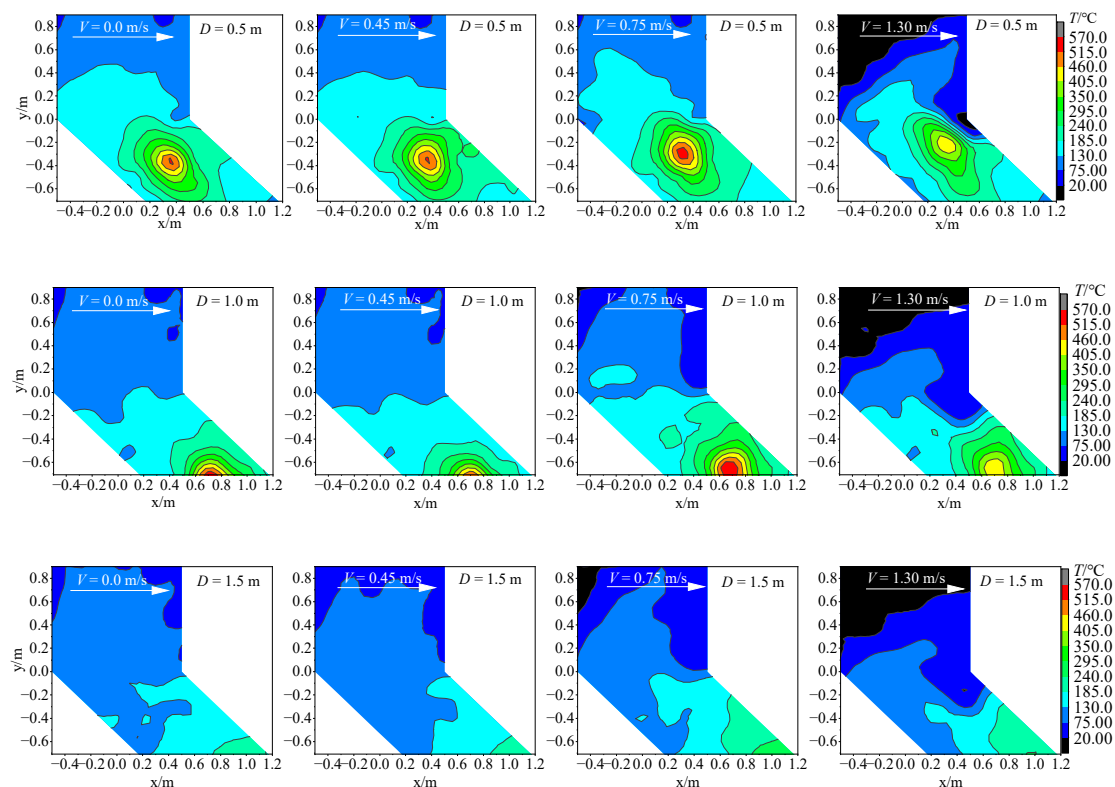


Figure 3. Temperature distribution in the bifurcation junction region for 15.9 kW conditions.

Figure 4 displays the temperature profile of smoke following the main tunnel roof for typical experimental conditions. Noticeably, the maximum temperature of smoke appears upstream of the main tunnel with no ventilation, whereas it gradually moves downstream with increasing ventilation velocity.

Notably, when longitudinal ventilation exists, the smoke temperature upstream of the junction in the main tunnel will be reduced to ambient temperature at a certain longitudinal location, and the larger the value of V , the smaller the distance of smoke temperature from ambient temperature. In addition, the smoke temperature downstream of the main tunnel junction decreases with increasing ventilation rates. Moreover, for fixed HRR and V , the temperature of smoke upstream and downstream of the junction in the main tunnel drops, as D increases.

Based on the description above, the smoke of a fire would spread in different directions after hitting the ceiling of the tunnel in question. When the longitudinal wind velocity in the tunnel is small, driven by the thermal buoyancy generated by the fire source, the ceiling jet upstream of the fire source moves along the ceiling against the longitudinal wind, forming a smoke countercurrent, which is a special fire phenomenon in tunnels. In previous works,

Tomas [47] proposed a model to evaluate the length of smoke back-layering in tunnels as follows:

$$L^* = \frac{L}{H} = \frac{gHQ}{\rho_0 c_p T_0 V^3 A} L^* \tag{4}$$

where L denotes the flame length; L^* denotes the dimensionless smoke back-layering length in the tunnel; Q is the total release rate of the fire, v is the longitudinal wind rate. According to previous works, the length of smoke back-layering in a tunnel is associated with the heat release rate Q of the fire and the longitudinal wind rate. It is worth noting that the length of smoke back-layering is positively associated with the rate of heat release from the fire, but negatively associated with the longitudinal wind velocity. But, the impact of the location of the fire source on the length of smoke back-layering was not mentioned.

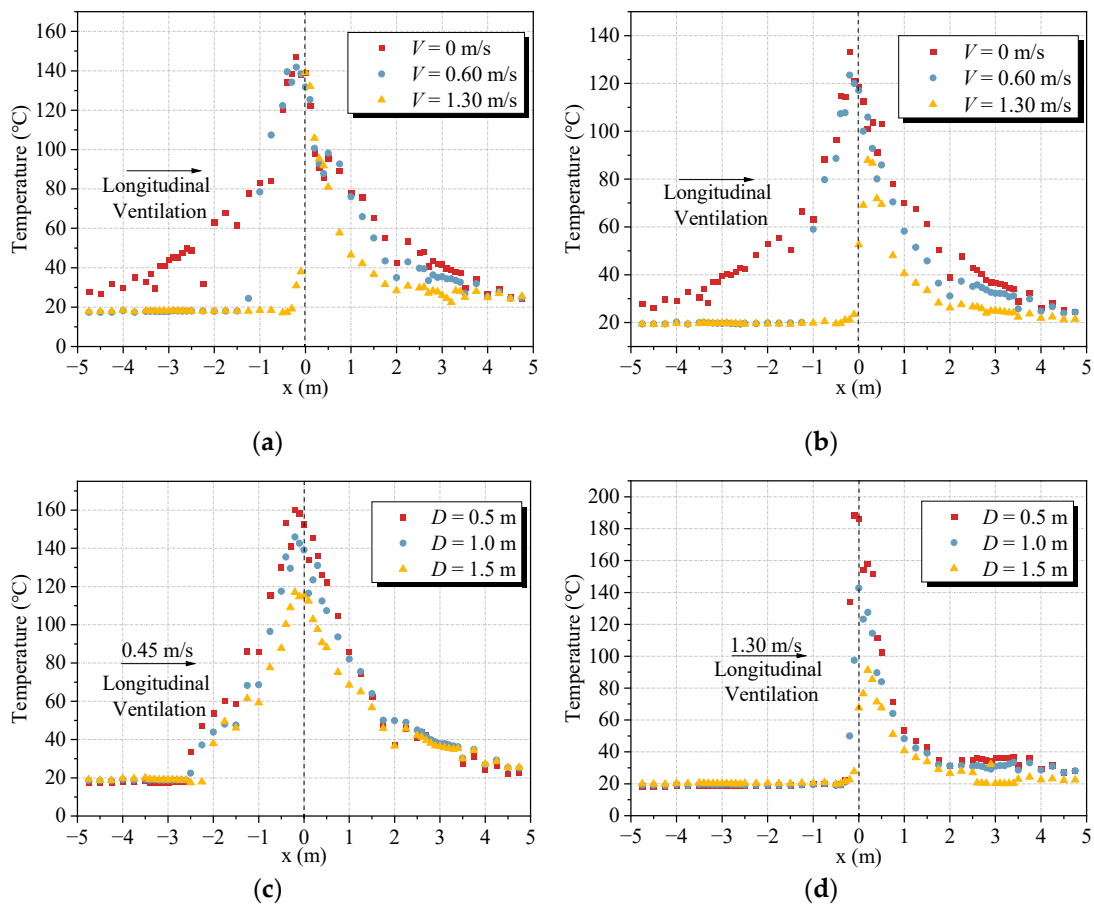


Figure 4. Distribution of longitudinal temperatures inside the main tunnel under typical experimental conditions: (a) HRR = 23.9 kW, $D = 0.5$ m; (b) HRR = 23.9 kW, $D = 1.0$ m; (c) HRR = 31.9 kW, $V = 0.45$ ms⁻¹; and (d) HRR = 31.9 kW, $V = 1.3$ ms⁻¹.

A relationship between the length of smoke back-layering, the longitudinal wind velocity, and the fire source’s location is plotted in Figure 5. It is observed from the figure that the length of the smoke back-layering in tunnel decreases following the increasing longitudinal wind velocity. In particular, a significant decrease in the length of smoke back-layering in the tunnel is observed for a longitudinal wind velocity between 0.4 to 0.75 ms⁻¹. Moreover, the increase in the length of the smoke back-layering in the tunnel is also noticed under condition of greater HRR of a fire. For example, for conditions of a 0.45 ms⁻¹ longitudinal wind velocity with a fire location at 0.5 m, the lengths of the smoke back-layering in the tunnel for 15.9 kW, 23.9 kW, and 31.9 kW are 2.61 m, 2.40 m, and 1.99 m, respectively. The experimental observation of a variation in the length of the smoke back-layering with the HRR of a fire and the longitudinal wind velocity in a tunnel fits the

results found in previous studies well. It is worth noting that the value of the length of the smoke back-layering decreases when the longitudinal fire location is far away from the main tunnel. As the distance of the location of the fire source and the main tunnel gets further away, the smoke in the bifurcation tunnel faces a greater along-travel resistance, and the rate of smoke spread is reduced. Consequently, the longitudinal wind velocity has a significant impact on the smoke entering the main tunnel under conditions of a larger fire location.

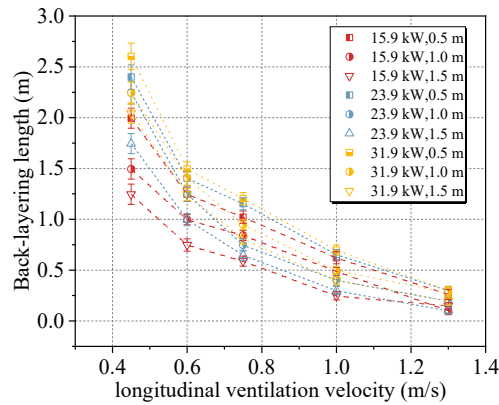


Figure 5. Variation in length of smoke back-layering in a tunnel with longitudinal ventilation velocity.

In Equation (4) the values of the coefficient of Q , H , ρ_0 , c_p , T_0 , and A are constant in this work. The relationship of L^* and Q/v^3 can be expressed as follows: $L^* \propto n \times \frac{Q}{v^3}$. The fitting results of coefficient n for different experimental conditions are shown in Figure 6. It can be noted that, as the fire source moves toward the intersection region, the coefficient n increases from 0.0069 to 0.0096, indicating that L^* is proportional to Q/v^3 , which is consistent with previous works by Tomas [47]. This may be attributed to the fact that the fire source is located in the branch tunnel, and only part of the smoke spreads into the main tunnel. The amount of smoke entering the main tunnel is reduced, and, therefore, the length of the smoke back-layering is shorter than that in a conventional tunnel.

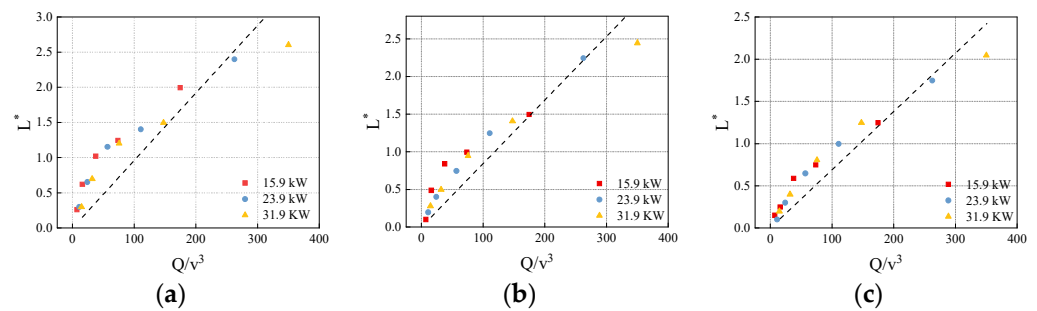


Figure 6. Relationship between L^* and Q/v^3 under different conditions: (a) 0.5 m; (b) 1.0 m; and (c) 1.5 m.

3.2. Smoke Temperature profile in a Main Tunnel

Evers and Waterhouse [48] proposed a formula for predicting the longitudinal temperature distribution in tunnel-like structures, shown as follows:

$$\frac{\Delta T_x}{\Delta T_{\max}} = k_1 e^{-k_2 x} \tag{5}$$

where ΔT_x indicates the rise in temperature at position x ; x indicates the distance from the measurement point to the reference point in the longitudinal direction; k_1 and k_2 are constant and can be obtained experimentally. Subsequently, Hu et al. [49] conducted

a number of fire experiments in a traditional single tunnel and established a modified correlation for calculating the smoke temperature profile, which can be expressed as follows:

$$\frac{\Delta T_x}{\Delta T_{max}} = e^{-kx} \tag{6}$$

where k is constant. Based on previous works [4,5,48,49], the dimensionless longitudinal smoke temperature profile is exponentially decreasing as a function of longitudinal distance. Figure 7 plots the dimensionless longitudinal smoke temperature profile downstream of the junction with conditions of various ventilation velocity for $D = 0.5$ m and $HRR = 15.9$ kW in the main tunnel, in which the exponentially fitted correlations are shown as black solid lines. The squared-correlation coefficients (R^2) are not less than 0.925, which indicates that the exponential law is appropriate for determining the dimensionless longitudinal smoke temperature attenuation in the main tunnel. The attenuation coefficient k increases with the longitudinal ventilation velocities and is significantly different from that for a fire source located in the main tunnel, as in the work of Li et al. [40].

Since the attenuation coefficient k when the source of the fire is situated in the branch tunnel differs to that of when the source of the fire is located in the main tunnel, it is necessary to study the variation of the attenuation coefficient k when the fire source is located in the branch tunnel. Moreover, the attenuation coefficient k for various longitudinal fire locations and ventilation velocities is summarized in Table 2 and Figure 8. It is noted that the attenuation coefficient k in the main tunnel increases noticeably with longitudinal ventilation velocity, but does not change significantly with longitudinal fire location. In this paper, a power law is applied to describe the relationship between the attenuation coefficient k and longitudinal ventilation velocity, as presented with the dotted solid line in Figure 8.:

$$k = 0.30V^{2.28} + 0.65 \tag{7}$$

Table 2. Attenuation coefficient k for various longitudinal fire locations and ventilation velocities in main tunnel.

Fire Location D (m)	Ventilation Velocity V (ms ⁻¹)					
	0.00	0.45	0.60	0.75	1.00	1.30
0.5	0.64	0.67	0.71	0.82	0.88	1.26
1.0	0.62	0.70	0.73	0.84	1.05	1.17
1.5	0.70	0.73	0.75	0.84	0.90	1.18

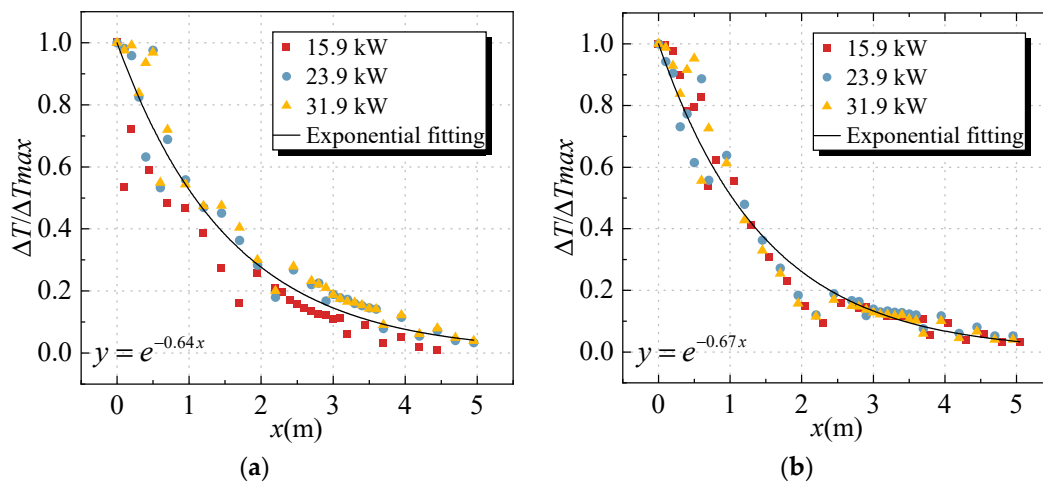


Figure 7. Cont.

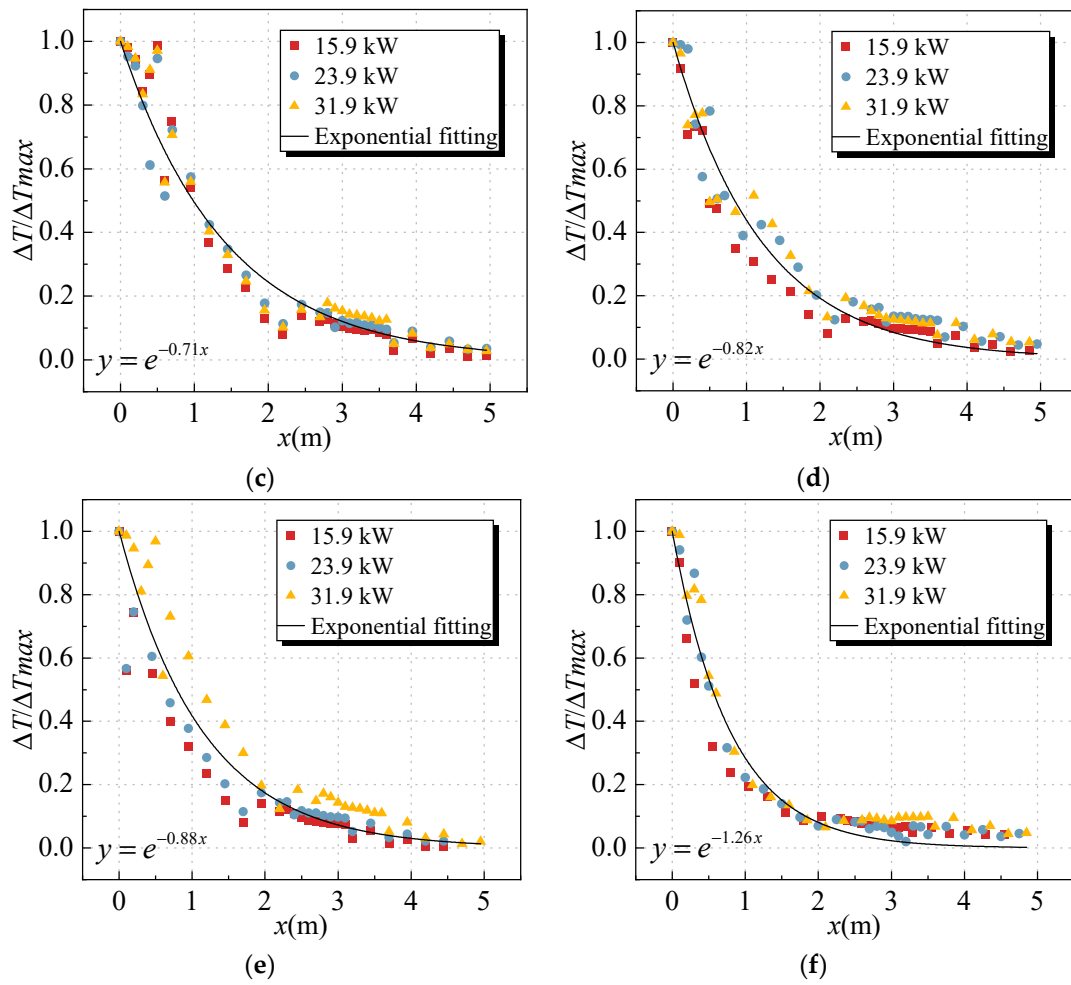


Figure 7. Distribution of smoke temperature downstream of the main tunnel junction for conditions of various ventilation velocities ($D = 0.5\text{ m}$, $\text{HRR} = 15.9\text{ kW}$): (a) $V = 0\text{ ms}^{-1}$; (b) $V = 0.45\text{ ms}^{-1}$; (c) $V = 0.6\text{ ms}^{-1}$; (d) $V = 0.75\text{ ms}^{-1}$; (e) $V = 1.0\text{ ms}^{-1}$; and (f) $V = 1.3\text{ ms}^{-1}$.

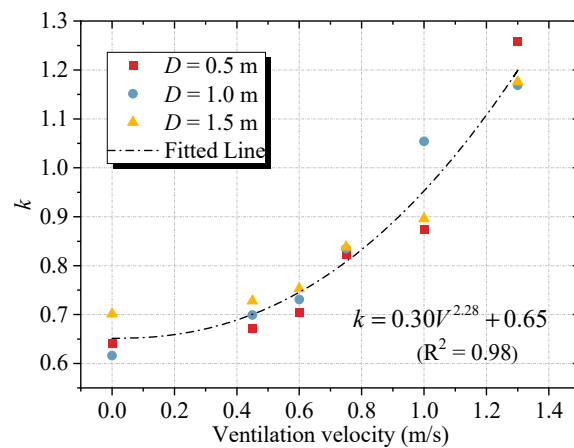


Figure 8. Attenuation coefficient k for various longitudinal fire locations and ventilation velocities in the main tunnel.

The R^2 is more than 0.94, demonstrating that the k increases with longitudinal ventilation velocity according to a power law. Substituting Equation (3) in Equation (2), the longitudinal smoke temperature profile downstream of the junction in the main tunnel can be determined using the following:

$$\frac{\Delta T_x}{\Delta T_{\max}} = e^{-(0.30V^{2.28} + 0.65)x} \quad (8)$$

Figure 9 plots the contrast between the experimental values and the predicted values of dimensionless longitudinal smoke temperature decay in the main tunnel according to the Equation (7) and the results of k . It is noted that the predicted values of longitudinal fire smoke temperature from a main tunnel fire fit the experimental data on smoke temperature well, which demonstrates that the model proposed in this work predicts longitudinal smoke temperature decay well.

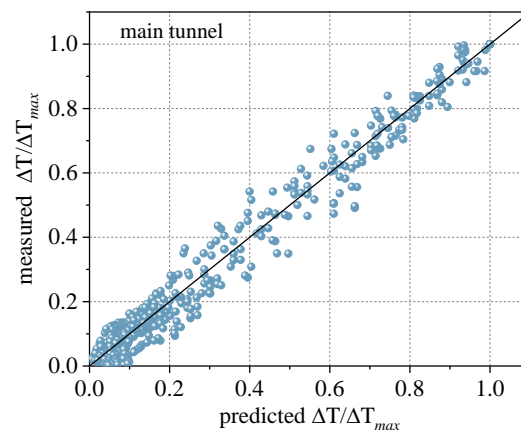


Figure 9. Comparison between the experimental values and the predicted values of dimensionless longitudinal attenuation of smoke temperature in the main tunnel.

3.3. Smoke Temperature Profile in a Branch Tunnel

Figure 10 shows the variations in the temperature profile of smoke as a function of longitudinal distance in the branch tunnel for typical experimental conditions. It is observed that the smoke temperature upstream or downstream of the fire site decreases as the longitudinal distance increases. Notably, when there is no ventilation, the variations in temperature attenuation upstream and downstream are noticeably different due to the branch structure, which is different from what is observed in a traditional single tunnel, where the smoke temperature up-stream or downstream of the fire source are essentially similar. Apparently, for fixed HRR and D , the smoke temperature profile downstream of the fire source drops as V rises, especially in the area around the fire source. Moreover, with constant values HRR and V , the maximum smoke temperature in the branch tunnel increases as the value of D increases, and the developments in the temperature profile along the longitudinal distance vary.

Figure 11 shows the dimensionless lengthwise smoke temperature curves downstream of the combustion source with conditions of various V for $D = 0.5$ m in the branch tunnel. The dimensionless smoke temperature profile downstream of the fire source can be seen to decrease exponentially with increasing longitudinal distance from the branch tunnel. However, most R-square degrees of exponential fitting for the dimensionless longitudinal temperature measured using Equation (2) are less than 0.85. Through theoretical analyses and experimental studies, Ji et al. [4] present a modified correlation method for determining the smoke temperature profile in tunnel structures as follows:

$$\frac{\Delta T_x}{\Delta T_{\max}} = ae^{-k'x} + b \quad (9)$$

where a and b are constant, which can be obtained by experiments. The results of an exponential fit to the dimensionless lengthwise temperature in the bifurcated tunnel using Equation (5) are plotted in Figure 11. The correlation coefficients of the fitted lines are all greater than 0.94, which indicates that Equation (5) can well reflect the dimensionless

temperature decay in the branch tunnel. The values of a , b , and k are summarized in Table 3.

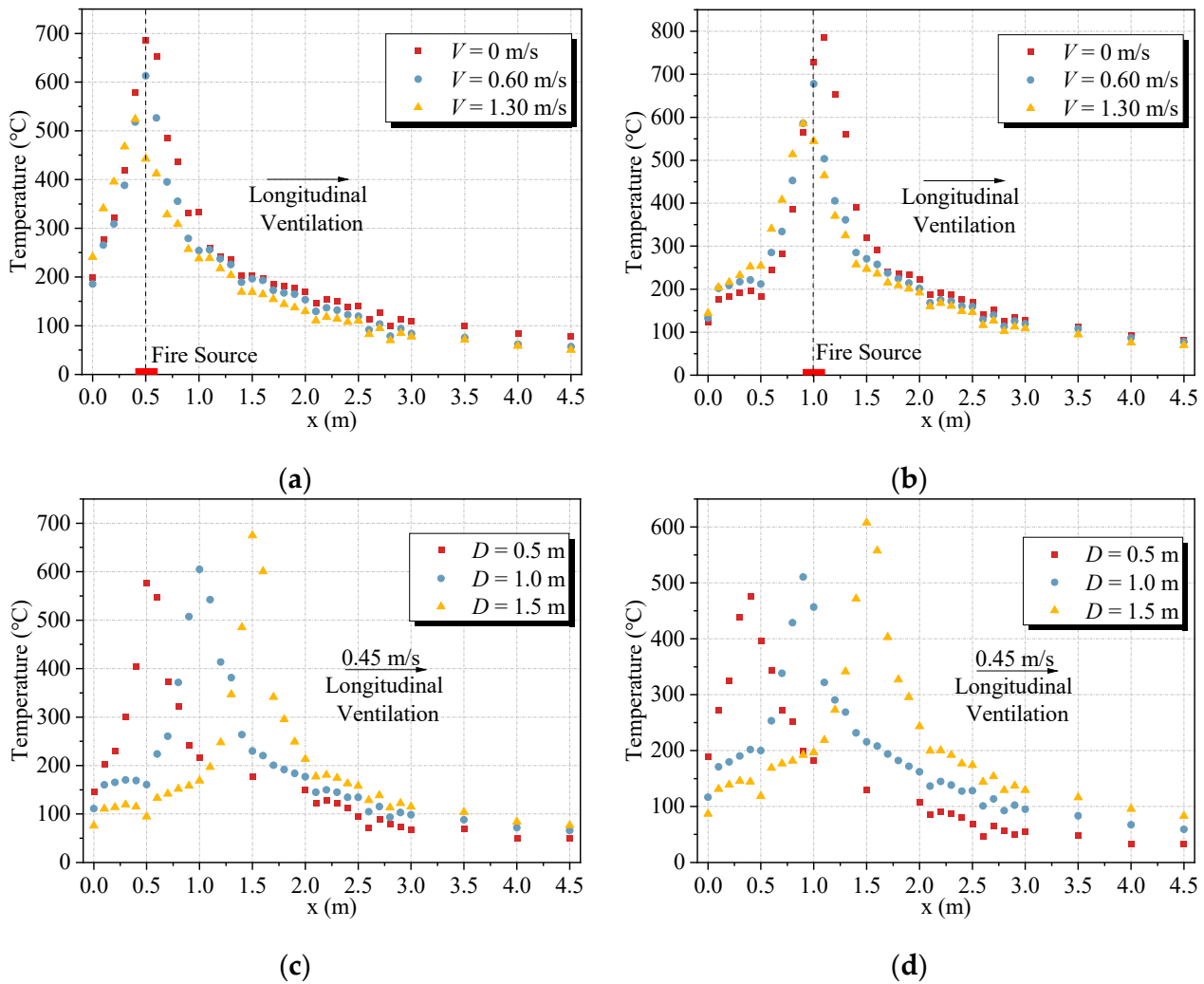


Figure 10. Smoke temperature profile in the branch tunnel for typical experimental conditions: (a) HRR = 31.9 kW, $D = 0.5$ m; (b) HRR = 31.9 kW, $D = 1.0$ m; (c) HRR = 23.9 kW, $V = 0.45$ ms⁻¹; and (d) HRR = 23.9 kW, $V = 1.30$ ms⁻¹.

Table 3. Fitting coefficients of a , b and k .

V (ms ⁻¹)	D=0.5 m			D=1.0 m			D=1.5 m		
	a	b	k	a	b	k	a	b	k
0.0	0.80	0.16	2.25	0.81	0.17	3.16	0.82	0.19	4.21
0.45	0.84	0.15	2.34	0.85	0.16	2.64	0.84	0.17	3.90
0.60	0.81	0.15	2.17	0.82	0.17	2.33	0.80	0.18	3.40
0.75	0.86	0.15	1.99	0.85	0.17	2.15	0.76	0.19	2.66
1.00	0.82	0.12	1.87	0.84	0.16	2.13	0.76	0.19	1.73
1.30	0.83	0.14	1.62	0.85	0.17	1.51	0.75	0.20	1.54
Average	0.83	0.15	×	0.84	0.17	×	0.78	0.19	×

According to Equation (8) and the fitting result of coefficients of a , b , and k , the predicted dimensionless lengthwise smoke temperatures for the bifurcated tunnel were calculated and compared to the experimental values, as shown in Figure 12. As seen in

the figure, the predicted data for the dimensionless lengthwise smoke temperature in the branch tunnel match very well with the smoke temperature observations made in this work.

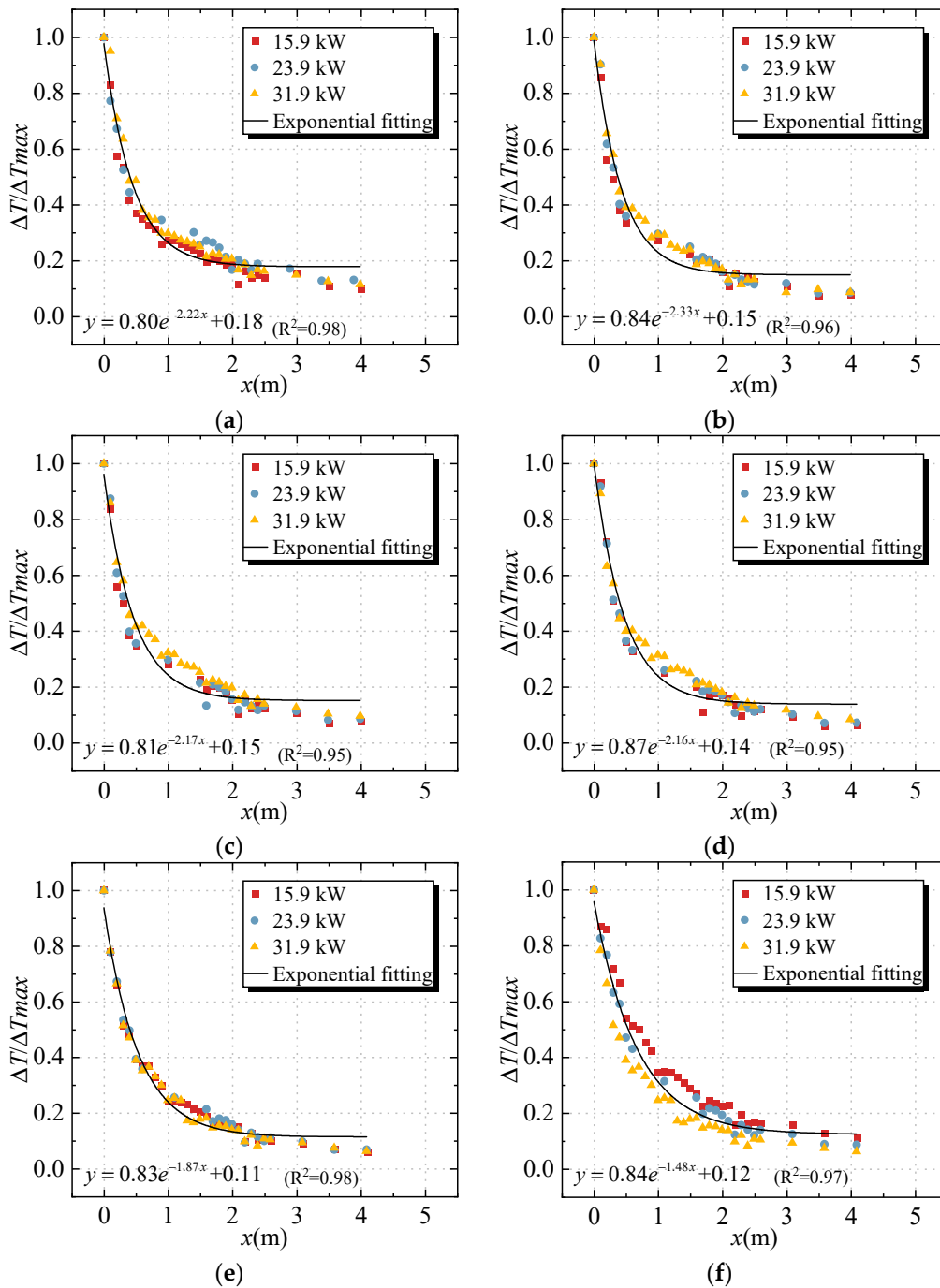


Figure 11. Longitudinal temperature attenuation fitting in a bifurcated tunnel (HRR = 15.9 kW): (a) $V = 0.0 \text{ ms}^{-1}$; (b) $V = 0.45 \text{ ms}^{-1}$; (c) $V = 0.6 \text{ ms}^{-1}$; (d) $V = 0.75 \text{ ms}^{-1}$; (e) $V = 1.0 \text{ ms}^{-1}$; and (f) $V = 1.3 \text{ ms}^{-1}$.

It is evident from Table 3 that, for fixed D, the values of a and b do not vary significantly with ventilation velocity, whereas the exponential coefficient of k' decreases with ventilation velocity overall. Noticeably, the average values of a and b for different fire locations change slightly around a constant value, which indicates that the fire source location does not have a significant influence on the values of a and b. Figure 13 presents the exponential coefficient k' with ventilation velocity for various fire location conditions. It is

noted that the exponential coefficient k' decreases with ventilation velocity, whereas the value of k' increases with longitudinal fire location in the branch tunnel. A linear fit is applied to describe the relationship between the exponential coefficient k' and ventilation velocity, which can be shown with the dotted line in Figure 13. Evidently, the linear fitting coefficients are related to the longitudinal fire location in the branch tunnel. By substituting the coefficients of a , b , and k' into Equation (5), a simplified model for predicting the temperature profile downstream of the fire source in a branch tunnel can be obtained, taking into account the ventilation rate and the longitudinal position of the fire source.

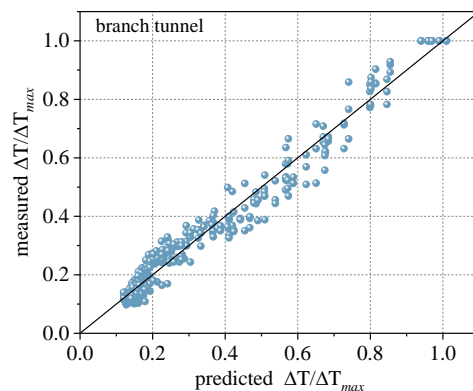


Figure 12. Comparison between the experimental values and the predicted data of dimensionless longitudinal smoke temperature attenuation in a bifurcated tunnel.

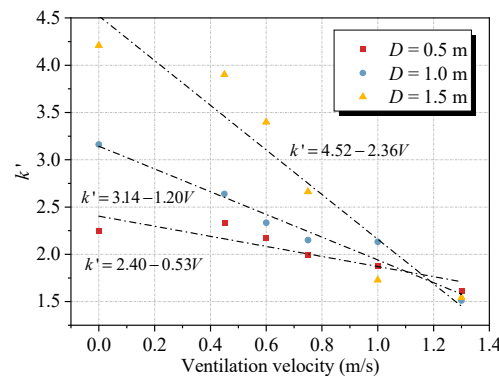


Figure 13. Exponential coefficient k' with ventilation velocity for various fire location conditions.

4. Conclusions

This experiment investigated the effects of ventilation rate and the position of longitudinal fires in a bifurcated tunnel on the smoke temperature distribution in said branch tunnel. The temperature profile of the smoke downstream of the main tunnel decreases with the ventilation rate and the location of the longitudinal ignition source. In addition, the smoke temperature profile downstream of the bifurcated tunnel fire decreases with the ventilation rate, but the maximum smoke temperature increases with the lengthways fire source position. The dimensionless smoke temperature decreases exponentially in both the main and bifurcated tunnels. The variations of the exponential attenuation coefficient in the main and bifurcated tunnels were quantitatively analyzed and revealed with respect to the fire location and ventilation velocity. Moreover, this paper proposed the modified model of smoke temperature distribution downstream of the main and bifurcated tunnels considering the effects of ventilation rate and fire source positioning. However, the angles of the main tunnel and the bifurcated tunnel have a significant effect on smoke flowing and temperature, which need to be investigated in order to gain a better understanding.

A further study is in progress to investigate the effects of bifurcation angle on flame behaviors and temperature profiles.

Author Contributions: Conceptualization, H.G. and Y.G.; data curation, Z.Y. and P.Z.; formal analysis, H.G.; investigation, H.G.; validation, Z.Y. and P.Z.; writing—original draft, H.G.; writing—review and editing, Y.G. and Y.Z. All authors have read and agreed to the published version of the manuscript.

Funding: This research was funded by the National Key R&D Program of China (2022YFC3801104), the National Natural Science Foundation of China (NSFC) (52278415 and 52108478), and Sichuan Science and Technology Program (2023YFS0407).

Data Availability Statement: The data presented in this study are available on request from the corresponding author.

Conflicts of Interest: The authors declare no conflict of interest.

References

1. Vuilleumier, F.; Weatherill, A.; Crausaz, B. Safety aspects of railway and road tunnel: Example of the Lötschberg railway tunnel and Mont-Blanc road tunnel. *Tunn. Undergr. Space Technol.* **2002**, *17*, 153–158. [[CrossRef](#)]
2. Lei, P.; Chen, C.; Zhang, Y.; Xu, T.; Sun, H. Experimental study on temperature profile in a branched tunnel fire under natural ventilation considering different fire locations. *Int. J. Therm. Sci.* **2021**, *159*, 106631. [[CrossRef](#)]
3. Alpert, R.L. Turbulent Ceiling-Jet Induced by Large-Scale Fires. *Combust. Sci. Technol.* **1975**, *11*, 197–213. [[CrossRef](#)]
4. Ji, J.; Fan, C.; Zhong, W.; Shen, X.; Sun, J. Experimental investigation on influence of different transverse fire locations on maximum smoke temperature under the tunnel ceiling. *Int. J. Heat Mass Transf.* **2012**, *55*, 4817–4826. [[CrossRef](#)]
5. Fan, C.; Ji, J.; Gao, Z.; Sun, J. Experimental study on transverse smoke temperature distribution in road tunnel fires. *Tunn. Undergr. Space Technol.* **2013**, *37*, 89–95. [[CrossRef](#)]
6. Delichatsios, M.A. The flow of fire gases under a beamed ceiling. *Combust. Flame* **1981**, *43*, 1–10. [[CrossRef](#)]
7. Hu, L.; Huo, R.; Wang, H.; Li, Y.; Yang, R. Experimental studies on fire-induced buoyant smoke temperature distribution along tunnel ceiling. *J. Affect. Disord.* **2007**, *42*, 3905–3915. [[CrossRef](#)]
8. Li, Y.Z.; Lei, B.; Ingason, H. The maximum temperature of buoyancy-driven smoke flow beneath the ceiling in tunnel fires. *Fire Saf. J.* **2011**, *46*, 204–210. [[CrossRef](#)]
9. Hu, L.; Chen, L.; Wu, L.; Li, Y.; Zhang, J.; Meng, N. An experimental investigation and correlation on buoyant gas temperature below ceiling in a slopping tunnel fire. *Appl. Therm. Eng.* **2013**, *51*, 246–254. [[CrossRef](#)]
10. Hu, L.; Huo, R.; Peng, W.; Chow, W.; Yang, R. On the maximum smoke temperature under the ceiling in tunnel fires. *Tunn. Undergr. Space Technol.* **2006**, *21*, 650–655. [[CrossRef](#)]
11. Hu, L.; Huo, R.; Chow, W. Studies on buoyancy-driven back-layering flow in tunnel fires. *Exp. Therm. Fluid Sci.* **2008**, *32*, 1468–1483. [[CrossRef](#)]
12. Bai, Z.P.; Li, Y.F. Effect of Longitudinal Ventilation on Smoke Temperature below Utility Tunnel Ceiling. *Eng. Lett.* **2020**, *28*, 939–943.
13. Zhao, S.; Liu, F.; Wang, F.; Weng, M. Experimental studies on fire-induced temperature distribution below ceiling in a longitudinal ventilated metro tunnel. *Tunn. Undergr. Space Technol.* **2018**, *72*, 281–293. [[CrossRef](#)]
14. Chen, C.-K.; Zhu, C.-X.; Liu, X.-Y.; Yu, N.-H. Experimental investigation on the effect of asymmetrical sealing on tunnel fire behavior. *Int. J. Heat Mass Transf.* **2016**, *92*, 55–65. [[CrossRef](#)]
15. Huang, Y.; Li, Y.; Dong, B.; Li, J.; Liang, Q. Numerical investigation on the maximum ceiling temperature and longitudinal decay in a sealing tunnel fire. *Tunn. Undergr. Space Technol.* **2018**, *72*, 120–130. [[CrossRef](#)]
16. Li, J.; Li, Y.; Li, J.; Yang, Q. Numerical investigation on the smoke behaviour and longitudinal temperature decay in tilted tunnel fire with portal sealing. *Indoor Built Environ.* **2023**, *32*, 133–148. [[CrossRef](#)]
17. Yuan, Z.Y.; Lei, B.; Bi, H.Q. The Effect of Fire Location on Smoke Temperature in Tunnel Fires with Natural Ventilation. *Procedia Eng.* **2015**, *121*, 2119–2124. [[CrossRef](#)]
18. Haddad, R.K.; Zulkifli, R.; Maluk, C.; Harun, Z. Experimental Investigation on the Influences of Different Horizontal Fire Locations on Smoke Temperature Stratification under Tunnel Ceiling. *J. Appl. Fluid Mech.* **2020**, *13*, 1289–1298.
19. Cong, W.; Shi, L.; Shi, Z.; Peng, M.; Yang, H.; Zhang, S.; Cheng, X. Effect of train fire location on maximum smoke temperature beneath the subway tunnel ceiling. *Tunn. Undergr. Space Technol.* **2020**, *97*, 103282. [[CrossRef](#)]
20. Sturm, P.; Föföleitner, P.; Fruhwirt, D.; Galler, R.; Wenighofer, R.; Heindl, S.F.; Krausbar, S.; Heger, O. Fire tests with lithium-ion battery electric vehicles in road tunnels. *Fire Saf. J.* **2022**, *134*, 103695. [[CrossRef](#)]
21. Álvarez-Coedo, D.; Ayala, P.; Cantizano, A.; Węgrzyński, W. A coupled hybrid numerical study of tunnel longitudinal ventilation under fire conditions. *Case Stud. Therm. Eng.* **2022**, *36*, 102202. [[CrossRef](#)]
22. Galhardo, A.; Viegas, J.; Coelho, P.J. The influence of wind on smoke propagation to the lower layer in naturally ventilated tunnels. *Tunn. Undergr. Space Technol.* **2022**, *128*, 104632. [[CrossRef](#)]
23. Li, Q.; Chen, C. Survey and measurement of the vehicle pollutant emission in urban underground bifurcate tunnel, China. *Sustain. Cities Soc.* **2019**, *48*, 101519. [[CrossRef](#)]
24. Li, Q.; Chen, C.; Yuan, H.; Wang, L.; Xu, S.; Li, Y. Prediction of pollutant concentration and ventilation control in urban bifurcate tunnel, China. *Tunn. Undergr. Space Technol.* **2018**, *82*, 406–415. [[CrossRef](#)]

25. Liu, C.; Zhong, M.; Tian, X.; Zhang, P.; Xiao, Y.; Mei, Q. Experimental and numerical study on fire-induced smoke temperature in connected area of metro tunnel under natural ventilation. *Int. J. Therm. Sci.* **2019**, *138*, 84–97. [[CrossRef](#)]
26. Tang, F.; Li, L.; Chen, W.; Tao, C.; Zhan, Z. Studies on ceiling maximum thermal smoke temperature and longitudinal decay in a tunnel fire with different transverse gas burner locations. *Appl. Therm. Eng.* **2017**, *110*, 1674–1681. [[CrossRef](#)]
27. Li, L.; Li, S.; Wang, X.; Zhang, H. Fire-induced flow temperature along tunnels with longitudinal ventilation. *Tunn. Undergr. Space Technol.* **2012**, *32*, 44–51. [[CrossRef](#)]
28. Chen, L.F.; Hu, L.H.; Zhang, X.L.; Zhang, X.Z.; Zhang, X.C.; Yang, L.Z. Thermal buoyant smoke back-layering flow length in a longitudinal ventilated tunnel with ceiling extraction at difference distance from heat source. *Appl. Therm. Eng.* **2015**, *78*, 129–135. [[CrossRef](#)]
29. Chen, L.; Hu, L.; Tang, W.; Yi, L. Studies on buoyancy driven two-directional smoke flow layering length with combination of point extraction and longitudinal ventilation in tunnel fires. *Fire Saf. J.* **2013**, *59*, 94–101. [[CrossRef](#)]
30. Thomas, P.H. The Movement of Smoke in Horizontal Passages against Air Flow. *Fire Saf. Sci.* **1968**, *7*, 1–8.
31. Zhong, W.; Li, Z.; Wang, T.; Liang, T.; Liu, Z. Experimental Study on the Influence of Different Transverse Fire Locations on the Critical Longitudinal Ventilation Velocity in Tunnel Fires. *Fire Technol.* **2015**, *51*, 1217–1230. [[CrossRef](#)]
32. Kurioka, H.; Oka, Y.; Satoh, H.; Sugawa, O. Fire properties in near field of square fire source with longitudinal ventilation in tunnels. *Fire Saf. J.* **2003**, *38*, 319–340. [[CrossRef](#)]
33. Wu, Y.; Bakar, M. Control of smoke flow in tunnel fires using longitudinal ventilation systems—A study of the critical velocity. *Fire Saf. J.* **2000**, *35*, 363–390. [[CrossRef](#)]
34. Lei, P.; Chen, C.; Jiao, W.; Shi, C. Experimental study on collaborative longitudinal ventilation of smoke control for branched tunnel fires considering different branch angles. *Tunn. Undergr. Space Technol.* **2023**, *136*, 105097. [[CrossRef](#)]
35. Chen, L.; Zhou, S.; Lan, Y.; Liu, X.; Yang, Y.; Li, X.; Yan, X.; Chen, H. Experimental study on fire characteristics of the bifurcated tunnel under multi-directional ventilation. *Int. J. Therm. Sci.* **2023**, *185*, 108072. [[CrossRef](#)]
36. Tao, H.; Xu, Z.; Zhang, Y.; Zhang, X.; Fan, C. An experimental study on the smoke spread in underground interconnected infrastructure with longitudinal ventilation. *Tunn. Undergr. Space Technol.* **2023**, *142*, 105381. [[CrossRef](#)]
37. Chen, C.; Nie, Y.; Zhang, Y.; Lei, P.; Fan, C.; Wang, Z. Experimental investigation on the influence of ramp slope on fire behaviors in a bifurcated tunnel. *Tunn. Undergr. Space Technol.* **2020**, *104*, 103522. [[CrossRef](#)]
38. Chen, C.; Zhang, Y.; Lei, P.; Zeng, W.; Jiao, W. Experimental study on fire behaviors in narrow bifurcated channel with a confined portal. *Combust. Sci. Technol.* **2020**, *193*, 2194–2216. [[CrossRef](#)]
39. Liu, C.; Zhong, M.; Shi, C.; Zhang, P.; Tian, X. Temperature profile of fire-induced smoke in node area of a full-scale mine shaft tunnel under natural ventilation. *Appl. Therm. Eng.* **2017**, *110*, 382–389. [[CrossRef](#)]
40. Li, Z.; Gao, Y.; Li, X.; Mao, P.; Zhang, Y.; Jin, K.; Li, T.; Chen, L. Effects of transverse fire locations on flame length and temperature distribution in a bifurcated tunnel fire. *Tunn. Undergr. Space Technol.* **2021**, *112*, 103893. [[CrossRef](#)]
41. Chen, L.; Mao, P.; Zhang, Y.; Xing, S.; Li, T. Experimental study on smoke characteristics of bifurcated tunnel fire. *Tunn. Undergr. Space Technol.* **2020**, *98*, 103295. [[CrossRef](#)]
42. Huang, Y.; Li, Y.; Li, J.; Li, J.; Wu, K.; Zhu, K.; Li, H. Experimental investigation on maximum gas temperature beneath the ceiling in a branched tunnel fire. *Int. J. Therm. Sci.* **2019**, *145*, 105997. [[CrossRef](#)]
43. Yang, X.; Luo, Y.; Li, Z.; Guo, H.; Zhang, Y. Experimental investigation on the smoke back-layering length in a branched tunnel fire considering different longitudinal ventilations and fire locations. *Case Stud. Therm. Eng.* **2021**, *28*, 101497. [[CrossRef](#)]
44. Li, Y.Z.; Ingason, H. Model scale tunnel fire tests with automatic sprinkler. *Fire Saf. J.* **2013**, *61*, 298–313. [[CrossRef](#)]
45. Li, Y.Z.; Lei, B.; Ingason, H. Study of critical velocity and backlayering length in longitudinally ventilated tunnel fires. *Fire Saf. J.* **2010**, *45*, 361–370. [[CrossRef](#)]
46. Ho, C.L.; Li, K.Y.; Spearpoint, M.J. Numerical simulation of scale-model smoke contamination of upper atrium levels by a channelled balcony spill plume. *Fire Mater.* **2012**, *37*, 581–596. [[CrossRef](#)]
47. Thomas, P. The movement of buoyant fluid against a stream and the venting of underground fires. *Fire Saf. Sci.* **1958**, *351*, 1.
48. Evers, E.; Waterhouse, A. A complete model for analyzing smoke movement in building. In *Building Research Establishment*; BRE CP: Borehamwood/Hertfordshire, England, 1981; Volume 69.
49. Hu, L.H.; Huo, R.; Li, Y.Z.; Wang, H.B.; Chow, W.K. Full-scale burning tests on studying smoke temperature and velocity along a corridor. *Tunn. Undergr. Space Technol.* **2005**, *20*, 223–229. [[CrossRef](#)]

Disclaimer/Publisher’s Note: The statements, opinions and data contained in all publications are solely those of the individual author(s) and contributor(s) and not of MDPI and/or the editor(s). MDPI and/or the editor(s) disclaim responsibility for any injury to people or property resulting from any ideas, methods, instructions or products referred to in the content.